

Multifrequency Continuous-Wave Radar Approach to Ranging in Passive UHF RFID

Daniel Arnitz, *Student Member, IEEE*, Klaus Witrisal, *Member, IEEE*, and Ulrich Muehlmann, *Member, IEEE*

Abstract—In this paper, we present the extension of a recently published two-frequency continuous-wave (CW) ultra-high-frequency RF identification ranging technique to multiple carriers. The proposed system concept relies on exact phase information; hence, the passive tag cannot be accurately modeled as a frequency-flat linear device. A linearized model of the tag's reflection coefficient is devised to bridge the gap between the nonlinear reality and the linear CW radar theory. Estimation error bounds are derived and effects caused by noise and multipath propagation are analyzed in detail. It has been found that systematic errors introduced by the tag's reflection characteristic cannot be compensated by using multiple carriers due to large variations caused by detuning. Nonetheless the system, while being vulnerable to multipath propagation effects, still performs well under line-of-sight conditions; mean average errors below 15% of the true distance are possible in typical fading environments.

Index Terms—Continuous-wave (CW) radar, detuning, multipath channel, narrowband, ranging, system modeling, ultra-high-frequency (UHF) RF identification (RFID).

I. INTRODUCTION

THE AUTOMATIC and simultaneous identification, localization, and tracking of targets using electromagnetic radiation started mainly as a military application in radar systems. In the early 1970s, commercial tracking of large and expensive goods emerged, followed by smaller items by the end of the 20th Century [1]. Since then, RF identification (RFID) became almost ubiquitous in commercial applications, e.g., tracking and identification of goods or electronic article surveillance.

Although estimating distances to tagged items is not a new idea in itself, it is a relatively new field of interest in passive ultra-high-frequency (UHF) RFID. Recent work combines the need for a continuous carrier (to power the tag) with range estimation, employing well-known principles like continuous-wave (CW) radar [2], [3]. The application of multiple carriers is also not a new idea in UHF RFID [4].

The restrictive spectral masks enforced by existing regulations are a major reason for using narrowband systems like amplitude modulation CW radar for ranging (cf. [5]). Wideband systems like frequency modulation CW radar and ultra-wideband (UWB) systems [6], [7] would require considerable modifications to existing regulations.

Manuscript received June 03, 2008; revised December 29, 2008. First published April 07, 2009; current version published May 06, 2009. This work was supported by NXP Semiconductors, Gratkorn, Austria, and by the Austrian Research Promotion Agency (FFG) under Grant 818072.

D. Arnitz and K. Witrisal are with the Signal Processing and Speech Communication Laboratory, Graz University of Technology, A-8010 Graz, Austria (e-mail: daniel.arnitz@tugraz.at; witrisal@tugraz.at).

U. Muehlmann is with NXP Semiconductors, A-8101 Gratkorn, Austria (e-mail: ulrich.muehlmann@nxp.com).

Digital Object Identifier 10.1109/TMTT.2009.2017320

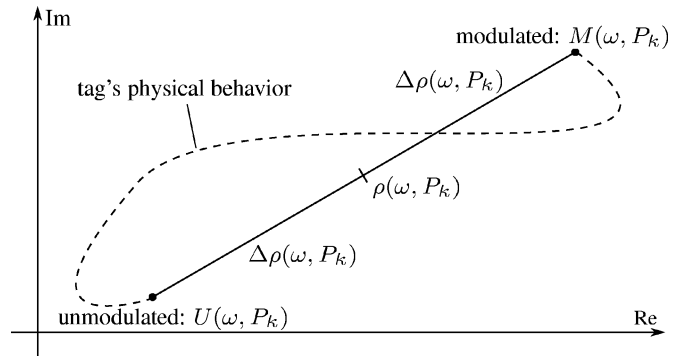


Fig. 1. Tag reflection coefficient linearization: the tag's physical behavior during modulation is a nonlinear, time-variant, frequency-dependent, and power-dependent curve. The linearized model assumes a fictive center value $\rho(\omega, P_\kappa)$ and a difference value $\Delta\rho(\omega, P_\kappa)$; only the endpoints are identical to the original curve. The assumption of short-time stationary power $P(\kappa) = P_\kappa$ completes the linearization.

This study completes the theoretical background of the recently published two-frequency continuous wave (2FCW) radar approach for passive UHF RFID [2]. This ranging system is also extended to multiple carriers in an effort to minimize errors introduced by noise, multipath propagation, and tag variations. The resulting multifrequency continuous-wave (MFCW) ranging approach is evaluated under typical UHF RFID environmental conditions.

In Section II, a linearized model of the tag's reflection coefficient during backscatter modulation is introduced. This model is applied in Section III to derive the signals used for MFCW ranging, followed by the derivation of a distance estimate out of multiple carriers and a discussion of detuning effects in Section IV. Section V contains detailed noise and multipath propagation influence analyses. The ranging system concept is verified using a wideband UHF RFID system-level simulator [8] in Section VI. Finally, the findings are summarized in Section VII.

II. LINEAR MODEL OF THE TAG MODULATION

On the physical level, a tag modulates data by varying a modulation impedance. The reflection coefficient during this process depends on the chip impedance, which itself depends on the chip input power. This dependence causes the reflection coefficient to be nonlinear. Moreover, the interaction between the time-variant impedances creates a curved transition trajectory in the complex plane (cf. Fig. 1). Tag detuning can be interpreted as additional impedance, thus having a direct influence on the reflection coefficient as well.

As a first step, the linearization neglects everything but the end points of this curve, introducing a center value $\rho(\omega, P)$ and

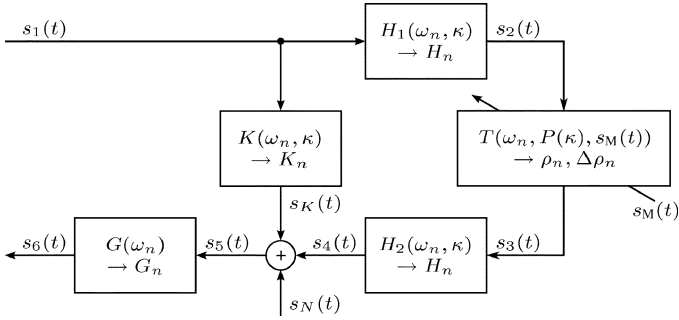


Fig. 2. Used signal model: reader to reader channel $K(\omega, \kappa)$, reader to tag channels $H_1(\omega, \kappa)$ and $H_2(\omega, \kappa)$, tag reflection coefficient $T(\omega, P, s_M(t))$, reader input stage $G(\omega)$, modulation signal $s_M(t)$, carrier level signals $s_1(t)$ through $s_6(t)$, noise $s_N(t)$; κ is a time index for short-time stationary variables, ω is the angular frequency, t is the time variable, and n is the carrier index.

a difference value $\Delta\rho(\omega, P)$ where ω and P are the angular frequency and the available tag power, respectively. The end points are more important here than the trajectory itself due to the nearly square tag modulation (either modulated or unmodulated)

$$\begin{aligned} \text{modulated : } & M(\omega, P) = \rho(\omega, P) + \Delta\rho(\omega, P) \\ \text{unmodulated : } & U(\omega, P) = \rho(\omega, P) - \Delta\rho(\omega, P). \end{aligned} \quad (1)$$

Assuming an arbitrary modulation signal $s_M(t)$ satisfying $-1 \leq s_M(t) \leq 1$, we can approximate the time-variant tag reflection coefficient $T(\omega, P, t)$ by

$$T(\omega, P, s_M(t)) \approx \rho(\omega, P) + s_M(t) \cdot \Delta\rho(\omega, P) \quad (2)$$

which is a simplified trajectory, but still power dependent, and thus, nonlinear. Under the assumption of short-time stationary power P_κ for some time period with index κ , the linearization is complete as follows:

$$T(\omega, P_\kappa, s_M(t)) \approx \rho_\kappa(\omega) + s_M(t) \cdot \Delta\rho_\kappa(\omega). \quad (3)$$

Note that ρ_κ and $\Delta\rho_\kappa$ still depend on carrier power, frequency, and detuning—they are merely linearized for one time instant.

As complex sinusoids are eigenfunctions of linear systems, we can finally write

$$e^{j\omega_n t} \cdot [\rho(\omega_n) + s_M(t) \cdot \Delta\rho(\omega_n)] \quad (4)$$

for the modulation of a sinusoid of frequency ω_n . The superposition principle is also applicable due to the linearity of this model, which will be exploited to calculate the backscattered signal for multiple carriers in Section III.

III. DERIVATION OF AMPLITUDE AND PHASE RELATIONS

The derivations outlined in this section are based on the signal model shown in Fig. 2 and done in the complex baseband. The entire derivation assumes short-time stationarity.

The interrogator sends $s_1(t)$ and receives $s_5(t)$. The sent signal is composed of N_c carriers at different frequency offsets ω_n from the center carrier. Phase relationships between the

carriers and the demodulation signal are implicitly considered in the carrier amplitudes A_n

$$s_1(t) = \sum_{n=1}^{N_c} A_n e^{j\omega_n t}. \quad (5)$$

Downlink and uplink channels are assumed to be linear filter channels, modeled by frequency-dependent gain factors H_n for purely sinusoidal signals

$$s_2(t) = \sum_{n=1}^{N_c} A_n H_n e^{j\omega_n t}. \quad (6)$$

Modulation on tag is performed using the linear model introduced in Section II. We assume a cosine modulation signal

$$s_M(t) = \cos(\omega_M t + \phi_M) = \frac{1}{2} e^{j(\omega_M t + \phi_M)} + \frac{1}{2} e^{-j(\omega_M t + \phi_M)} \quad (7)$$

where ω_M is the modulation frequency and ϕ_M is an arbitrary phase shift. We use the superposition principle to calculate the backscattered signal

$$\begin{aligned} s_3(t) = & \sum_{n=1}^{N_c} A_n H_n \rho_n e^{j\omega_n t} + \frac{1}{2} \sum_{n=1}^{N_c} A_n H_n \Delta\rho_n e^{j((\omega_n + \omega_M)t + \phi_M)} \\ & + \frac{1}{2} \sum_{n=1}^{N_c} A_n H_n \Delta\rho_n e^{j((\omega_n - \omega_M)t - \phi_M)}. \end{aligned} \quad (8)$$

Uplink and downlink channels are assumed to be identical for simplicity, but can easily be separated in the results. If the channels are not identical [distinct transmit and receive antennas (cf. [9])], only the average distance can be estimated.

The feedback term $s_K(t)$ models direct coupling caused by parasitics and nonideal devices, as well as reflections by the channel. Like uplink and a downlink channels, it is modeled as linear filter channel that decomposes into frequency-dependent gain factors K_n for sinusoidal signals

$$s_K(t) = \sum_{n=1}^{N_c} A_n K_n e^{j\omega_n t}. \quad (9)$$

The received signal $s_5(t)$ consists of modulated carriers $s_4(t)$, unmodulated carriers $s_K(t)$, and additive noise $s_N(t)$. We will denote the n th carrier's upper sideband by index $n + M$, while the lower sideband is denoted $n - M$. For example, the channel gain H_{4+M} is the gain for the upper sideband of carrier $n = 4$. Finally, the reader frontend introduces an additional frequency-dependent gain factor G . Hence,

$$\begin{aligned} s_6(t) = & s_N(t) + \sum_{n=1}^{N_c} A_n G_n (K_n + H_n^2 \rho_n) e^{j\omega_n t} \\ & + \frac{1}{2} \sum_{n=1}^{N_c} A_n H_n H_{n+M} G_{n+M} \Delta\rho_n e^{j((\omega_n + \omega_M)t + \phi_M)} \\ & + \frac{1}{2} \sum_{n=1}^{N_c} A_n H_n H_{n-M} G_{n-M} \Delta\rho_n e^{j((\omega_n - \omega_M)t - \phi_M)}. \end{aligned} \quad (10)$$

We extract the deterministic channel delay τ from the channel gains, e.g.,

$$H_{n+M} = \tilde{H}_{n+M} \cdot e^{-j(\omega_c + \omega_n + \omega_M)\tau} \quad (11)$$

with ω_c being the carrier frequency. The phase of the remaining channel gain \tilde{H}_{n+M} is completely stochastic, reflecting multipath propagation.

The frequency components of $s_6(t)$ are separated by shifting each component to dc and applying a low-pass filter (direct conversion receiver). We define the complex amplitude of the n th carrier's upper sideband as

$$c_{n+M} := \frac{1}{2} A_n \tilde{H}_n \tilde{H}_{n+M} G_{n+M} \Delta \rho_n e^{j[\phi_M - \tau \cdot (2\omega_c + 2\omega_n + \omega_M)]} \quad (12)$$

and the amplitude of the corresponding lower sideband as

$$c_{n-M} := \frac{1}{2} A_n \tilde{H}_n \tilde{H}_{n-M} G_{n-M} \Delta \rho_n e^{-j[\phi_M + \tau \cdot (2\omega_c + 2\omega_n - \omega_M)]} \quad (13)$$

for $n = 1, \dots, N_c$. Estimates of these amplitudes are used by MFCW ranging to determine the distance to the tag.

IV. MFCW DISTANCE ESTIMATE

The set of lower and upper sideband phases $\angle c_{n+M}$ and $\angle c_{n-M}$ form a system of equations that is solved for the desired delay τ . Estimation based on the received signal strength (RSS) is also possible, but not in the scope of this paper.

The tag modulation phase shift ϕ_M is typically unknown and cannot be controlled by an interrogator or tag. It is thus assumed to be uniformly distributed between $-\pi$ and π . Since $\omega_c \gg \omega_n \gg \omega_M$, a direct solution of this system of equations leads to an ill-conditioned problem. Therefore, we subtract the phase shifts in order to eliminate ϕ_M and ω_c beforehand. This cannot be achieved by combining upper and lower sidebands, hence, c_{n+M} and c_{n-M} are used separately.

A phase comparison between two different components $i+M$ and $j+M$ in (12) or $i-M$ and $j-M$ in (13) leads to the following result; in short notation,

$$\begin{aligned} \angle c_{i\pm M} c_{j\pm M}^* &= \angle c_{i\pm M} - \angle c_{j\pm M} \\ &= 2\tau(\omega_j - \omega_i) + \angle \Delta \rho_i \Delta \rho_j^* \\ &\quad + \angle \tilde{H}_i \tilde{H}_{i\pm M} \tilde{H}_j^* \tilde{H}_{j\pm M} + \angle A_i A_j^* \\ &\quad + \angle G_{i\pm M} G_{j\pm M}^*. \end{aligned} \quad (14)$$

The last two terms $\angle A_i A_j^*$ and $\angle G_{i\pm M} G_{j\pm M}^*$ are systematic influences and can be compensated. Fading channels are represented by $\angle \tilde{H}_i \tilde{H}_{i\pm M} \tilde{H}_j^* \tilde{H}_{j\pm M}$. The effect of this term will be discussed in Section V; it is zero for additive white Gaussian noise (AWGN) channels. The differential phase shift caused by the tag $\angle \Delta \rho_i \Delta \rho_j^*$ is another error term and will be discussed below.

A distance estimate can be obtained from each comparison (14) by

$$\hat{d}_{i,j,\pm} = \frac{c}{2(\omega_j - \omega_i)} \angle \hat{c}_{i\pm M} \hat{c}_{j\pm M}^*, \quad i, j = 1, \dots, N_c, i \neq j \quad (15)$$

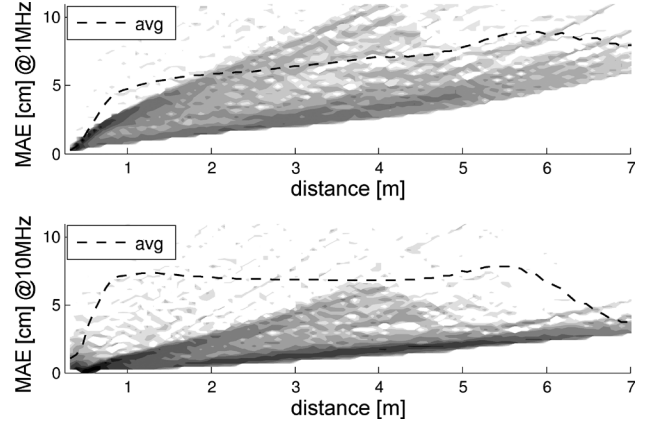


Fig. 3. Influence of detuning on the MAE for 2FCW ranging at frequency offsets of 1 and 10 MHz.

where c is the speed of light and $\hat{c}_{n\pm M}$ denotes an estimate of $c_{n\pm M}$. These estimates are averaged to obtain the desired overall distance.

A. Example: 2FCW Radar ($N_c = 2$)

Using two carriers and assuming perfectly compensated systematic errors, the phase shifts between the two upper and lower sidebands are identical

$$\angle c_{1+M} c_{2+M}^* = \angle c_{1-M} c_{2-M}^* = 2\tau(\omega_2 - \omega_1) + \angle \Delta \rho_1 \Delta \rho_2^* \quad (16)$$

and the distance estimate is

$$\hat{d} = \underbrace{\tau c}_d + \underbrace{\frac{c \cdot \angle \Delta \rho_1 \Delta \rho_2^*}{2(\omega_2 - \omega_1)}}_{\text{error caused by tag}}. \quad (17)$$

The error term introduced by the tag causes the distance estimate \hat{d} to be biased.

B. On Mitigation of the Systematic Error Caused by the Tag

The bias in (17) depends on frequency, power, and detuning. Exemplarily, this influence on the mean absolute error (MAE) of 2FCW ranging is shown in Fig. 3. Detuning plus assembly impedance is varied from -70% to 400% from the optimal value for this plot. We used an AWGN channel with single-sided noise density $N_0 = -82$ dBm/Hz and an estimation window size of $N = 144432$ samples. The carriers were set to 3.2 W/32 mW effective isotropic radiated power (EIRP) at a center frequency of $\omega_c = 910$ MHz with 0-Hz offset for the primary (energy) carrier. Note that the maximum range of detuned tags is considerably lower than 7 m; only functional tags are taken into account. The background of Fig. 3 contains a histogram of the MAE, while the foreground shows the average MAE. We have chosen a strong secondary carrier to minimize the influence of noise in these plots.

While noise is still an issue compared to the systematic bias for a frequency offset of 1 MHz and distances of >2 m, it is almost negligible for 10-MHz offset. The maximum MAE was approximately 40–50 cm for both plots, while the average MAE does not exceed 10 cm.

Effective removal of this error is a nontrivial task and yet unresolved. The tag is designed to work for a frequency range of 860–960 MHz specified in the EPCglobal Class-1 Gen-2 standard [10]. Consequently, its spectral characteristic is a smooth function and a Taylor-series expansion of the phase shift $\Delta\rho_i\Delta\rho_j^*$ is approximately linear subject to the frequency difference $(\omega_j - \omega_i)$ for reasonably small carrier offset frequencies. Since the phase shift caused by wave propagation $2\tau(\omega_j - \omega_i)$ is also linear with frequency difference, the effects of tag and distance cannot be separated using multiple carriers.

A characterization of the labels after manufacture and/or after application to the tagged items would tremendously increase costs and is thus not practicable. Moreover, such a characterization would lose its validity if the items are placed near other objects due to changes in the state of detuning. For the same reasons, i.e., the dependence of the error on individual incident power levels and on detuning, reference estimates based on tags at known ranges can only be used to compensate for an approximate average value, not for the true value. If the range of detuning is known, at least an expected average error can be compensated.

It shall be noted that typical UHF RFID channels are fading channels. The MAE is dominated by multipath propagation effects even in moderate multipath environments, not by detuning (cf. Fig. 9).

V. INFLUENCE OF NOISE AND MULTIPATH PROPAGATION

A. Influence of White Noise

Analogous to other phase estimators [11] and under the assumption of independent real and imaginary parts, i.e., circular symmetric noise, we can write

$$\text{var}\{\hat{\varphi}_i\} = \frac{1}{N \text{SNR}_i} = \frac{N_0}{N|c_i|^2} \quad (18)$$

for the variance of one phase estimate. N is the length of the estimation window in samples, N_0 is the single-sided noise density, and $|c_i|$ is the signal (component) amplitude. For the phase difference between two components, we obtain

$$\text{var}\{\hat{\varphi}_{ij}\} = \frac{1}{N \text{SNR}_i} + \frac{1}{N \text{SNR}_j} + \frac{r_{ij}}{N^2 \text{SNR}_i \text{SNR}_j} \quad (19)$$

where r_{ij} is the cross covariance between components i and j . Typically passive RFID systems are forward-link-limited [1] so signal-to-noise (SNR) values are high. It follows that the quadratic cross correlation term is negligible. Using (15) to obtain the distance results in

$$\text{var}\{\hat{d}_{ij}\} = \frac{c^2}{4(\omega_j - \omega_i)^2} \text{var}\{\hat{\varphi}_{ij}\}. \quad (20)$$

There are $N_c(N_c - 1)$ feasible combinations of phase differences between the sidebands of N_c carriers. Averaging all these combinations comes at the cost of correlation between the components. For the conservative approach of using each sideband only once, $\lfloor N_c \rfloor_e$ combinations remain, where $\lfloor N_c \rfloor_e$ denotes

the rounding to the next lower even integer value. For this case, we obtain

$$\begin{aligned} \text{var}\{\hat{d}\} &= \frac{c^2 N_0}{4N \lfloor N_c \rfloor_e^2} \sum_{i=1}^{N_c/2} \frac{|\hat{c}_{2i-1+M}|^2 + |\hat{c}_{2i+M}|^2}{|\hat{c}_{2i+1+M}|^2 |\hat{c}_{2i+M}|^2 (\omega_{2i} - \omega_{2i-1})^2} \\ &+ \frac{c^2 N_0}{4N \lfloor N_c \rfloor_e^2} \sum_{i=1}^{N_c/2} \frac{|\hat{c}_{2i-1-M}|^2 + |\hat{c}_{2i-M}|^2}{|\hat{c}_{2i+1-M}|^2 |\hat{c}_{2i-M}|^2 (\omega_{2i} - \omega_{2i-1})^2} \end{aligned} \quad (21)$$

for the overall variance. Remarkably, we can ignore the correlation between \hat{d}_{ij} and combine all sidebands in case of equal carrier amplitudes A_2, \dots, A_{N_c} (A_1 can be arbitrary) and equal frequency spacings, obtaining an approximation

$$\text{var}\{\hat{d}\} \approx \frac{1}{N_c^2 (N_c - 1)^2} \sum_{i=1}^{N_c} \sum_{\substack{j=1 \\ j \neq i}}^{N_c} \text{var}\{\hat{d}_{ij}\} \quad (22)$$

with

$$\hat{d}_{ij}|_{i>j} = \frac{c}{2} \cdot \frac{\angle \hat{c}_{i+M} \hat{c}_{j+M}^*}{(\omega_j - \omega_i)} \quad \hat{d}_{ij}|_{i<j} = \frac{c}{2} \cdot \frac{\angle \hat{c}_{i-M} \hat{c}_{j-M}^*}{(\omega_j - \omega_i)}. \quad (23)$$

Clearly, $N_c^2(N_c - 1)^2 \gg \lfloor N_c \rfloor_e^2$ for $N_c > 2$, thus the resulting variance is considerable lower if all sidebands are combined and the correlation can be neglected. The average component variance in such a system is approximately equal to the individual secondary carrier variances because of the strong primary (energy) carrier

$$\begin{aligned} \text{var}\{\hat{d}_{23}\} &= \text{var}\{\hat{d}_{32}\} = \text{var}\{\hat{d}_{34}\} = \dots \\ &\approx \overline{\text{var}\{\hat{d}_{ij}\}} = \frac{1}{N_c(N_c - 1)} \sum_{i=1}^{N_c} \sum_{\substack{j=1 \\ j \neq i}}^{N_c} \text{var}\{\hat{d}_{ij}\} \end{aligned} \quad (24)$$

It follows that the best achievable variance scaling for multiple carriers is

$$\text{var}\{\hat{d}\}|_{\text{MFCW}} \approx \frac{\overline{\text{var}\{\hat{d}_{ij}\}}}{N_c(N_c - 1)}. \quad (25)$$

while the largest possible frequency offset is $N_c \Delta\omega$ with $\Delta\omega$ being the frequency spacing. If this offset is chosen for 2FCW, according to (15), its variance scales with

$$\text{var}\{\hat{d}\}|_{2\text{FCW}} \approx \frac{\overline{\text{var}\{\hat{d}_{ij}\}}}{N_c^2}. \quad (26)$$

which is lower than the multicarrier's variance. Simulations have shown that the correlation can be used to reduce the variance caused by noise slightly below this level for multicarrier systems.

B. Influence of Multipath Propagation

In case of multipath propagation, the stochastic channel phase term $\angle \tilde{H}_i \tilde{H}_{i \pm M} \tilde{H}_j^* \tilde{H}_{j \pm M}^*$ in (14) is nonzero. We start our analysis with one channel, assuming given channel gains $\tilde{H}_i, \tilde{H}_j \sim \mathcal{CN}(m, \sigma^2)$, circular symmetric around the mean value. This assumption implies a Ricean fading channel with line-of-sight

(LOS) amplitude m and is valid for a small frequency spacing. We assume a pure smallscale channel here to strip the tilde and define the covariance matrix

$$\mathbb{E}\{\underline{h}\underline{h}^H\} - \mathbb{E}\{\underline{h}\}\mathbb{E}\{\underline{h}\}^H = \begin{bmatrix} \sigma^2 & \beta \\ \beta^* & \sigma^2 \end{bmatrix} \quad (27)$$

with $\underline{h} = [H_i \ H_j]^T$. The superscript H denotes the Hermitian transpose.

We are evaluating $\angle H_i - \angle H_j = \angle H_i H_j^*$ for the distance estimate, which is approximately

$$\angle H_i H_j^* = \arctan\left(\frac{\text{Im}\{H_i H_j^*\}}{\text{Re}\{H_i H_j^*\}}\right) \approx \frac{\text{Im}\{H_i H_j^*\}}{\text{E}\{\text{Re}\{H_i H_j^*\}\}} \quad (28)$$

for LOS scenarios with a high Ricean K-factor. Thus,

$$\text{var}\{\angle H_i H_j^*\} \approx \frac{\text{var}\{\text{Im}\{H_i H_j^*\}\}}{\text{E}\{\text{Re}\{H_i H_j^*\}\}^2}. \quad (29)$$

After some short derivations using the properties of complex Gaussian processes [12], we obtain

$$\mathbb{E}\{H_i H_j^*\} = \beta + |m|^2 \quad (30)$$

$$\text{var}\{\text{Im}\{H_i H_j^*\}\} = \frac{1}{2} \text{Re}\{\sigma^4 - \beta^2 + 2|m|^2(\sigma^2 - \beta)\} \quad (31)$$

and, thus,

$$\text{var}\{\angle H_i H_j^*\} \approx \frac{\text{Re}\{\sigma^4 - \beta^2 + 2|m|^2(\sigma^2 - \beta)\}}{2\text{Re}\{\beta + |m|^2\}^2} \quad (32)$$

which is the variance caused by one channel.

Introducing a second channel, we have to deal with $\angle H_i H_{i\pm M} H_j^* H_{j\pm M}^*$ instead of $\angle H_i H_{j\pm M}$, which is a lot more complicated to handle. The problem becomes simple if we assume that the product $H_i H_{i\pm M}$ is also approximately Gaussian with new variance and mean value $H_i H_{i\pm M} \sim \mathcal{CN}(\tilde{m}, \tilde{\sigma}^2)$. In this case, the above derivations apply to $H_i H_{i\pm M}$ as well. This assumption of Gaussianity holds for LOS scenarios with a high K-factor $K \gtrsim 10$ dB. Exploiting the properties of complex Gaussian processes again, it can easily be shown that

$$\tilde{m} = m^2 \quad \tilde{\sigma}^2 = 2\sigma^2(\sigma^2 + 2|m|^2) \quad \tilde{\beta} = 2\beta(\beta + 2|m|^2) \quad (33)$$

for identical uplink and downlink channels and

$$\tilde{m} = m^2 \quad \tilde{\sigma}^2 = \sigma^2(\sigma^2 + 2|m|^2) \quad \tilde{\beta} = \beta(\beta + 2|m|^2) \quad (34)$$

for distinct channels under this assumption.

The simplest way to obtain the variance for the combination of multiple carriers is to use the average frequency shift to calculate the covariance matrix. This approach is possible because of the small frequency spacings up to a few megahertz. Direct application of (21) is not possible due to heavy correlation between the phase estimates.

C. MAE

The expected MAE of the proposed ranging system concept can be expressed by mean and standard deviation of the calcu-

lated estimate. We assume a Gaussian distribution for the distance estimate \hat{d} , which is approximately true for LOS scenarios, i.e., high Ricean K-factors. Applying this assumption, the deviation from the true value d is also Gaussian with mean value $\mu := \mathbb{E}\{\hat{d}\} - d$ and the MAE is

$$\begin{aligned} \text{MAE}\{\hat{d}\} &= \mathbb{E}\{|\hat{d} - d|\} \\ &= \frac{1}{\sigma\sqrt{2\pi}} \int_{-\infty}^{\infty} |x - \mu| e^{-\frac{x^2}{2\sigma^2}} dx \\ &= \sqrt{\frac{2}{\pi}} \sigma e^{-\frac{\mu^2}{2\sigma^2}} + \mu \text{erf}\left\{\frac{\mu}{\sqrt{2}\sigma}\right\} \end{aligned} \quad (35)$$

where $\text{erf}\{\alpha\}$ is the error function [13]

$$\text{erf}\{\alpha\} = \frac{2}{\sqrt{\pi}} \int_0^{\alpha} e^{-x^2} dx. \quad (36)$$

VI. SIMULATIONS

A. Simulator Setup

The theoretical results given in this paper have been verified by simulations using a wideband interrogator/tag simulation tool [8]. It is based on behavioral models of tag and interrogator building blocks and partially implements the EPCglobal Class-1 Gen-2 protocol [10].

The simulator was configured as follows: carrier frequency $f_c = 910$ MHz, tag clock frequency $f_{\text{clk}} = 1.92$ MHz, and modulation frequency $f_M = 48$ kHz with an unknown uniformly distributed phase shift $\varphi_M \in [-\pi, \pi]$. Unless otherwise stated, transmit power of the primary (energy) carrier $n = 1$ was set to 3.2 W EIRP at a frequency offset of $f_1 = 0$ Hz, while secondary (ranging) carriers were set to 320 μ W EIRP. The average direct feedback gain was chosen to be $\mathbb{E}\{K_n\} = -30$ dB with an average delay of 3 ns; the sampling window size was set to $N = 144432$ samples for all simulations. Systematic errors that could be corrected by the interrogator in real-world applications are perfectly compensated.

The simulator results in Figs. 5–9 were calculated by averaging 250 independent estimates per marker. Four-frequency continuous-wave (4FCW) ranging was performed by comparing the phases of carriers 1/2 and 3/4 (each carrier used only once).

All simulated multipath channels are based on a short-range indoor smallscale channel model [14], resulting in Ricean fading. Uplink and downlink channels were chosen to be identical (worst case, cf. Fig. 8). All multipath simulations, except for Figs. 4 and 9, where a light fading channel was desired, used a logarithmically dropping Ricean K-factor with 30 dB at 0 m and 10 dB at 5 m. The root mean square (rms) delay spread increased logarithmically from 1 to 20 ns in the same range. This channel setup reflects the values given in the literature for the UHF RFID frequency band (cf. [9] and [15]). We extended the range to 7 m for the light fading channel, approximately resulting in an rms delay spread of 1–10 ns and a Ricean K-factor of 30–15 dB within 0–5 m. Additive white noise was set to -82 dBm/Hz after sampling at the reader input stage.

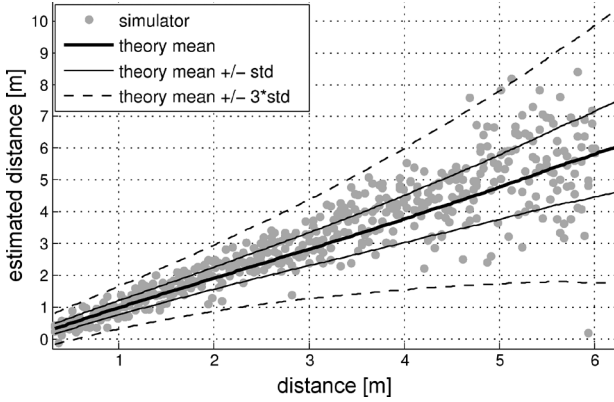


Fig. 4. Example comparison between analytical and simulation results for a weakly fading channel.

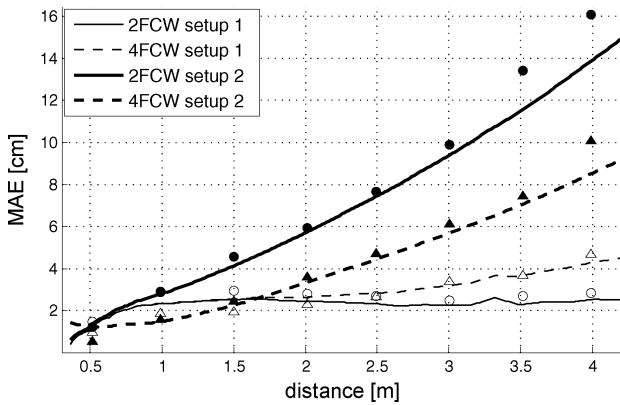


Fig. 5. Mean absolute distance error caused by **noise and the bias introduced by the tag** for 2FCW ($N_c = 2$) and 4FCW ($N_c = 4$): analytical results versus simulation for two different carrier setups. Carrier offset frequencies $f_n = 0, 3, 1, 2$ MHz (setup 1) and $f_n = 0, 4, 2, 10$ MHz (setup 2).

B. Simulation Results

The proposed ranging method was tested under various conditions of which only a small selection of simulations can be presented here.

Fig. 4 shows a comparison of theory and simulations for 2FCW radar using a frequency spacing of 8 MHz. In this simulation a detuned tag (+100% of the optimal impedance) moves from 30 cm to 6 m in the light multipath environment, while the interrogator continuously estimates its range. The expected average deviation using (17) and 68/99.7% intervals applying the results in Section V are also displayed for comparison. As can be seen, the ranging performs within expected parameters.

The MAE in AWGN and fading environments for different carrier setups is depicted in Figs. 5 and 6, respectively. Setup 2 uses the standard power setup, while the secondary carrier power is increased to $P_{2...4} = 32$ mW for Setup 1. All simulations assume a well-tuned tag; frequency setups are given in the captions. The small deviations from the expected analytical values given in this paper are caused by overlapping harmonics due to nonideal filters and residual filter transients. The results

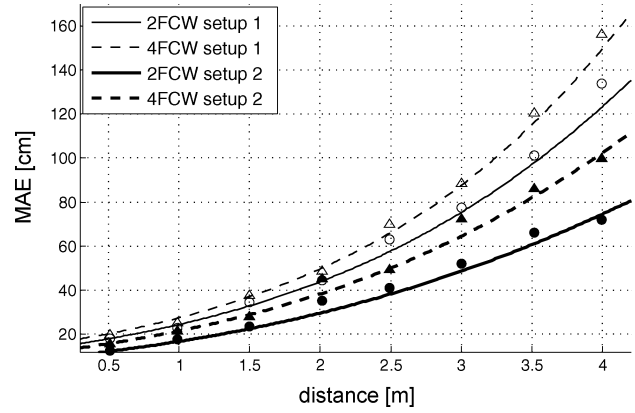


Fig. 6. Mean absolute distance error caused by **multipath propagation** for 2FCW ($N_c = 2$) and 4FCW ($N_c = 4$): analytical results versus simulation for two different carrier setups. Carrier offset frequencies $f_n = 0, 6, 2, 4$ MHz (setup 1) and $f_n = 0, 12, 2, 6$ MHz (setup 2).

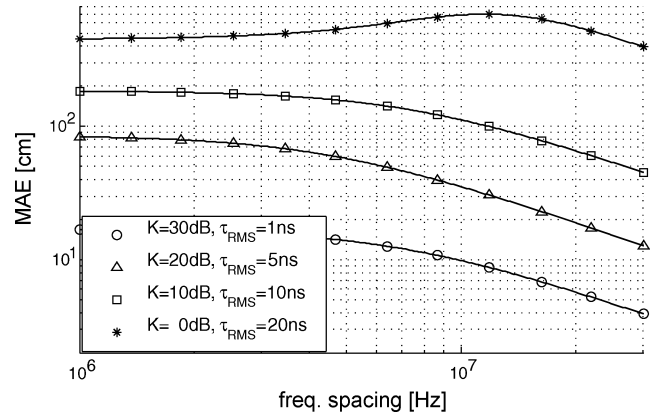


Fig. 7. Analytical mean absolute distance error caused by multipath propagation for 2FCW ($N_c = 2$) versus frequency spacing $f_2 - f_1$ for four different channels. Uplink/downlink channels are identical (worst case).

show that the performance depends primarily on the largest frequency offset. Moreover, noise is negligible compared to the errors caused by multipath propagation.

A special property of the proposed ranging system is shown in Fig. 7. The MAE for multipath propagation drops for an increased frequency spacing, as long as the channel features a significant LOS component. The maximum frequency offset is bounded by phase ambiguities at one quarter of the wavelength. We thus suggest to select the frequency offset of a 2FCW system such that

$$f_2 - f_1 \lesssim \frac{c}{4(d_{\max} + 3\sigma)} \quad (37)$$

where c is the speed of light, d_{\max} is the maximum distance, and σ is the standard deviation caused by the channel. This minimizes the influence of noise and multipath propagation while still avoiding phase ambiguities.

An undesired effect is caused by the combination of backscatter communication with identical receive/transmit (RX/TX) antenna at the interrogator. This combination creates identical uplink and downlink channels, increasing the fading range and the error rate of MFCW ranging, as shown in Fig. 8.

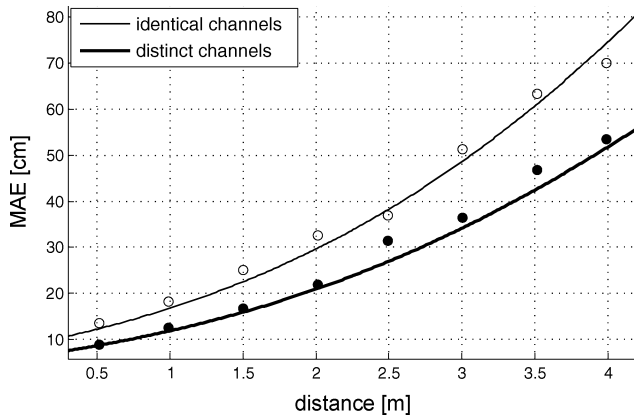


Fig. 8. Mean absolute distance error caused by **multipath propagation** for 2FCW ($N_c = 2$) using a well-tuned tag: analytical results versus simulation for identical and independent uplink/downlink channels.

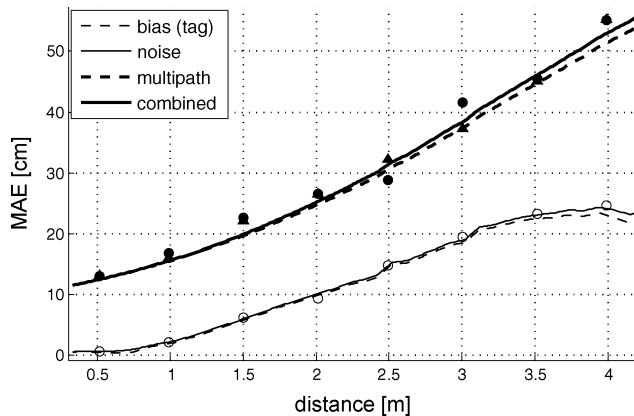


Fig. 9. Mean absolute distance error caused by **noise and multipath propagation** for 2FCW ($N_c = 2$): tag detuned by +100% of the optimal impedance, light multipath channel; carrier offset frequencies $f_n = 0, 10$ MHz.

This simulation uses offset frequencies of $f_n = 0, 12$ MHz and identical parameters per uplink and downlink channel. Analytical results are given in Section V.

A direct comparison between the errors caused by noise, multipath propagation, and the bias introduced by the tag's phase shift can be found in Fig. 9. We set up a simulation using only a moderate multipath channel with high K-factor and low rms delay spread for this plot. The tag is detuned by +100% of the optimal impedance, which approximately maximizes the influence of the bias on the MAE. Further detuning flattens the reflection coefficient and thus reduces the introduced error. It can be seen that the bias is dominant in the AWGN case, while it is almost negligible in the presence of multipath propagation.

VII. CONCLUSION

A linearized model of the time-variant nonlinear reflection coefficient of a passive UHF RFID tag was introduced in this paper. This model was designed for the EPCglobal Class-1 Gen-2 protocol standard [10], but is also applicable to other types of RFID transponders using backscatter modulation. The 2FCW radar ranging approach for UHF RFID presented in [2] was generalized to an arbitrary amount of carriers, utilizing an improved method of component selection. The resulting system

was analyzed for vulnerabilities to systematic and stochastic errors. Performance bounds for AWGN and multipath propagation channels were derived accordingly. The theoretical results were verified by extensive simulations using a wideband UHF RFID simulator [8].

It has been found that the system, while being vulnerable to multipath propagation (like any narrowband system), still performs well for typical RFID channels. The mean average error can be kept below 20% at distances from 0.75 m up to 4 m in such channels for the worst case of identical reader RX/TX-antennas. Using distinct antennas, the error can be kept well below 15% within the same range.

Detuning is a problem at short ranges and in nonfading channels. Simulations have shown that the MAE can exceed 50 cm for "unlucky" detuning, shifting the resonance exactly to the tag's operating point. The mean MAE for detuning in the range of -70% to 400% of the optimal impedance does not exceed 10 cm. Compensation of this error is not possible due to large variations caused by the detuning.

Finally, it has also been found that there is no gain in using more than one secondary carrier within the coherence bandwidth of the channel. As mentioned above, the systematic error caused by detuning could not be compensated using multiple carriers. Additionally, the estimate's variance cannot be improved using multiple secondary carriers inside the coherence bandwidth: In this case, the error caused by multipath propagation solely depends on the average carrier spacing, with smaller errors for larger offsets. If the 2FCW system uses the largest spacing, the variance for higher order systems is always greater than the 2FCW's variance. For AWGN channels, a similar relationship has been shown in Section V. Thus, the best achievable MAE is obtained when using 2FCW ranging with the highest possible frequency offset. Consequently, 2FCW radar is the recommended choice for narrowband ranging. Placing 2FCW carrier pairs well outside the respective coherence bandwidths will create independent fading and, thus, mitigate multipath propagation effects—at the cost of a considerably larger overall bandwidth.

REFERENCES

- [1] D. M. Dobkin, *The RF in RFID*. New York: Elsevier, 2007, 13: 978-0750682091.
- [2] U. Muehlmann and A. Salfelner, "Two-frequency CW RADAR approach to ranging in UHF RFID systems," in *Proc. Eur. Microw. Assoc.*, Dec. 2007, vol. 4, pp. 317–322.
- [3] M. Vossiek and P. Gulden, "The switched injection-locked oscillator: A novel versatile concept for wireless transponder and localization systems," *IEEE Trans. Microw. Theory Tech.*, vol. 56, no. 4, pp. 859–866, Apr. 2008.
- [4] H.-C. Liu, Y.-T. Chen, and W.-S. Tzeng, "A multi-carrier UHF passive RFID system," in *Int. Appl. Symp. and Internet Workshops*, Munich, Germany, Jan. 2007, p. 21.
- [5] K. Finkenzerler, *RFID Handbook: Fundamentals and Applications in Contactless Smart Cards and Identification*, 2nd ed. New York: Wiley, 2003, 13: 978-0470844021.
- [6] I. Oppermann, M. Hämmäläinen, and J. Iinatti, *UWB Theory and Applications*. New York: Wiley, 2004, 13: 978-0470869178.
- [7] Z. Sahinoglu, S. Gezici, and I. Guvenc, *Ultra-Wideband Positioning Systems: Theoretical Limits, Ranging Algorithms, and Protocols*. Cambridge, U.K.: Cambridge Univ. Press, 2008, 13: 978-0521873093.
- [8] D. Armitz, U. Muehlmann, T. Gigl, and K. Witrisal, "Wideband system-level simulator for passive UHF RFID," in *Proc. IEEE Int. RFID Conf.*, Orlando, FL, Apr. 2009, to be published.

- [9] D. Kim, M. A. Ingram, and W. W. Smith, "Measurements of small-scale fading and path loss for long range RF tags," *IEEE Trans. Antennas Propag.*, vol. 51, no. 8, pp. 1740–1749, Aug. 2003.
- [10] *EPCglobal Class 1 Gen 2*, ISO/IEC 18000-6C, ISO Standard, 2004.
- [11] S. M. Kay, *Fundamentals of Statistical Signal Processing—Estimation Theory*. New York: Prentice-Hall, 1993, vol. 1, 13: 978-0133457117.
- [12] K. S. Miller, *Complex Stochastic Processes*. Reading, MA: Addison-Wesley, 1974.
- [13] I. N. Bronstein, K. A. Semendjajew, G. Musiol, and H. Muehlig, *Taschenbuch der Mathematik* (in German), 5th ed. Berlin, Germany: Harri Deutsch, 2005, 10: 978-3817120154.
- [14] K. Witrisal, Y.-H. Kim, and R. Prasad, "A new method to measure parameters of frequency-selective radio channels using power measurements," *IEEE Trans. Commun.*, vol. 49, no. 10, pp. 1788–1800, Oct. 2001.
- [15] M. S. Varela and M. G. Sánchez, "RMS delay and coherence bandwidth measurements in indoor radio channels in the UHF band," *IEEE Trans. Veh. Technol.*, vol. 50, no. 2, pp. 515–525, Mar. 2001.



Daniel Arnitz (S'08) received the Master degree Dipl.-Ing.(FH) in electrical engineering from the University of Applied Sciences FH Joanneum Kapfenberg, Styria, Austria, in 2005. His diploma thesis focused on a feasibility study of (burst) error correcting codes for long-range RFID systems. He is currently working toward the Ph.D. degree at Graz University of Technology, Graz, Austria.

He is currently with the Signal Processing and Speech Communication Laboratory (SPSC), Graz University of Technology.



Klaus Witrisal (S'98–M'03) received the Dipl.-Ing. degree in electrical engineering from the Technical University of Graz, Graz, Austria, in 1997, and the Ph.D. degree (*cum laude*) from the Delft University of Technology, Delft, The Netherlands, in 2002. His doctoral thesis concerned frequency-domain channel characterization and orthogonal frequency division multiplexing (OFDM) transmission technology.

He is currently an Assistant Professor with the Signal Processing and Speech Communication Laboratory (SPSC), Graz University of Technology, Graz, Austria. His current research interests concern broadband wireless communications, in particular UWB technology, propagation channel modeling, and multiple-input–multiple-output (MIMO) systems.

Dr. Witrisal is co-chair of the Austria chapter of the IEEE Communications (COM)/Microwave Theory and Techniques (MTT) societies.



Ulrich Muehlmann (M'05) received the Dipl.-Ing. degree (Master) in telematics and Ph.D. degree (with honors) from the Graz University of Technology, Graz, Austria, in 2000 and 2005, respectively.

In 2001, he began research in optical tracking with the Department of Electrical Measurement and Measurement Signal Processing, Technical University of Graz, Graz, Austria). Since 2005, he has been with NXP Semiconductors (formerly Philips Semiconductors), Gratkorn, Austria, where he is involved with the field of UHF RFID technology focused on systems

and analog innovation. He has authored or coauthored several publications in the field of optical tracking, machine vision, and RFID.